https://doi.org/10.1016/j.jmatprotec.2019.05.007

Study on size effect affected progressive microforming of conical flanged parts directly using sheet metals

J.Y. Zheng, H.P. Yang, M.W. Fu*, C. Ng

Department of Mechanical Engineering, The Hong Kong Polytechnic University, Hung Hom, Kowloon, Hong Kong

** Email: mmmwfu@polyu.edu.hk*

Abstract

Progressive forming of microparts directly using sheet metals is an efficient approach for realization of mass production. However, there are many unknown behaviors and phenomena affecting the decision-making in process and tooling design, because the specimen generally comprises only a few grains in the wall thickness, where the mechanical response and deformation of material behave differently compared with those in macro-scale due to size effects. In this research, a progressive forming system including punching, extrusion, and blanking operations with three-scaled punches and dies was developed to fabricate cylindrical parts and conical flanged parts by directly using copper sheets with different grain sizes. Through physical experiments, measurement and analysis of the deformations and related variables, grain and specimen size effects affected deformation behaviors and the characteristics of the conical flanged parts were comprehensively studied in term of deformation pressure, microstructural evolution, dimensional accuracy, undesirable geometries and surface qualities. It is revealed from the experimental results that the forming pressure increases with the decrease of specimen and grain size. For the cylindrical parts, their scaled length increases with the decrease of grain size and increase of scaling factor. For the conical flanged parts, four deformation zones were

divided based on microstructural evolution. Properly coarse grains can reduce the undesirable geometries, but at a slight cost of deterioration of the quality of the formed conical surface. When scaled down to micro-scale, the undesirable geometries and the surface qualities deteriorate considerably. A worse forming quality appeared on the conical surface, where the defects including microcracks, microbulges, and micropits were observed. All these understandings facilitate the fabrication of conical flanged microparts directly using sheet metal in the aspects of deformation behaviors and controlling product qualities and enrich the knowledge of this unique microforming process.

Keywords: Progressive microforming, Micro bulk forming of sheet-metals, Size effect, Undesirable deformation.

1. Introduction

As the tendency of product miniaturization grows in microelectronics, biomedical and other industrial clusters, microparts used in various products are getting more and more popular (Geiger et al., 2001). For this demand, micromanufacturing technologies have been developed, and among them, microforming is a promising method to produce microparts. Engel and Eckstein (2002) defined microforming as the fabrication of metallic microparts or structures with at least two dimensions in sub-millimeter range for microsystem or microelectromechanical system (MEMS). Fu and Chan (2013b) considered microforming as a promising micromanufacturing process for its high productivity, less material waste, net-shape or near-net-shape characteristic and the advanced mechanical performance of final microparts.

However, the experience of macroforming is not competely applicable to the production of microparts because of size effect (Vollertsen et al., 2009). There are many issues including deformation behaviors, damage accumulation and deformation defects in microforming, which could be the barriers to mass production of microparts. To address these size effect induced issues in microforming, prior investigations have been conducted. Kim et al. (2007) developed a model combined specimen and grain size effects based on the hypothesis that the properties of polycrystal material would restore to those in single crystal when the individual grain size is increased to specimen size. Lin et al. (2015) designed a punch with a micro-ridged surface for the improvement of micro/meso-deep drawing formability. Gao et al. (2015) revealed that the size effects can influence formed height, forming force and distribution of micro-hardness in the roll-to-plate micro/meso-imprinting process. Zhang and Dong (2016) investigated the size effect and crystallographic orientation affected micro-tension of polycrystalline material considering crystal plasticity theory. Ran et al. (2013) examined the origin of ductile fracture in material deformation under micro-scale and established a model considering surface layer model combined with size effect for prediction of the ductile fracture. Wang et al. (2017) further conducted tensile and compression tests to investigate the ductile fracture attributed to size effect and stress condition by developing a size-dependent surface layer model. Cheng and Lee (2018) revealed the grain size and strain rate effects affected material formability by conducting limit dome height tests. Xu et al. (2018) studied the springback affected by the punch angle and the specimen and grain size effect in micro/meso-bending processes.

Nevertheless, the wide application of microforming in mass production is still obustructed by problems in handling, transporting and ejection. In addition, there are

some other critical issues such as the control of the dimensional accuracy of microparts and the assurance of product quality. To deal with the above-mentioned issues and improve the industrial efficiency to meet the growing requirements of mass production of microparts, the concept of progressive microforming has arisen and matured gradually. This microforming process is recognized as one of the most efficient forming processes to produce microparts by using progressive tools and sheet metals. One or more specific features are formed by the corresponding dies in each progressive forming operation. After a specific forming chain, a finished part with various features is produced and then blanked from the metal strip. Originally, Hirota (2007) used a novel approach to manufacture micro-pin parts through extruding the material in thickness direction. Fu and Chan (2013; 2013a) studied the feasibility of manufacturing cylindrical and flanged parts by directly using sheet metals and employing punching and extrusion operations in micro- and meso- scales. The characteristics of the complete parts and the deformation behaviors in the forming process were examined considering size effects. Ghassemali et al. (2013a; 2015; 2013b) used the extrusion process to fabricate micro-pin parts and investigated the material flow behavior considering the specimen and grain size effects. Meng et al. (2015a; 2015b; 2018) extensively explored the progressive microforming processes of cylindrical, double-flanged, and variable-thickness-flanged microparts and investigated the micromechanical damage related to grain size effect and forming conditions in the progressive microforming process.

Although several categories of progressive microparts were fabricated and studied, there is still lack of research on conical flanged microparts. The conical flanged parts are not only widely used as fastening parts for the function of sealing and preventing screw loosening, such as pipe joints and bolts, but also applied to flow controllers in

hydraulic systems. To solve screw loosening problems in product miniaturization and to develop micro- or meso-scaled hydraulic systems, how to efficiently fabricate micro-scaled conical flanged microparts is critical. In this paper, the flanged parts with the conical and cylindrical surfaces in three scales represented by scaling factors were fabricated by four operations, viz., punching, two steps of extrusion, and blanking. The deformation stages represented by the load-stroke curves in extrusion were classified and the four microstructure zones in the deformed flanged parts were identified. Moreover, the forming qualities and the characteristics of parts related to size effect were examined to explore size effects on the progressive forming process. It is revealed that the coarse-grained material has lower forming pressure, less undesirable geometries, and reduced quantities of dimples near the shearing surface, but slight deterioration of the conical surface quality is caused. However, the overlarge grain size results in grain cracks, which could affect the strength and other properties of the fabricated microparts. The findings enrich the knowledge and understanding in design of microparts, microforming process and tooling.

2. Experimental details

2.1 Preparation of test material

Pure copper was chosen as the test material in the experiment due to its great mechanical properties in manufacturing. The pure copper sheets with the thickness of 0.5, 1.0 and 1.5mm were used and they were annealed with diverse temperatures and holding time to obtain different grain sizes, viz., 500℃ for 2h, 600℃ for 3h and 750℃ for 2h. Then the copper sheets were cooled down to indoor temperature gradually in the furnace. Every annealing process was conducted in an argon gas-filled furnace to prevent oxidation. The detailed microstructures in the

cross-section along thickness direction and their average grain sizes (G) are shown in **Fig. 1**. The pictures of microstructures in specimens were taken by an optical microscope. The solution of $FeCl_3$ with dilute hydrochloric acid was used to etch the polished surface for 10 to 20 seconds. In addition, the grain sizes of specimens were measured based on the ASTM E112 standard.

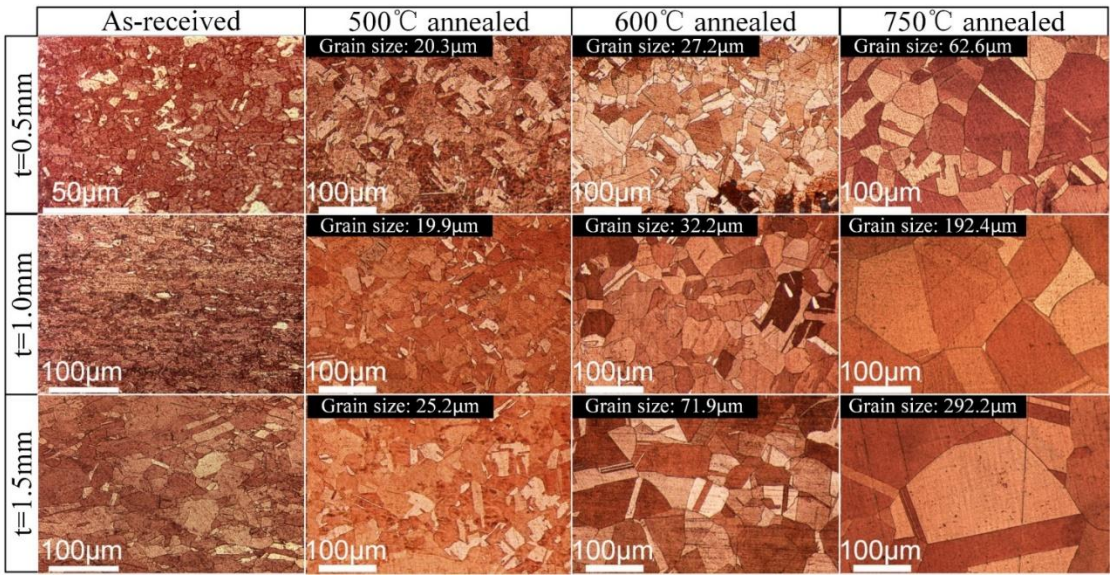

Fig. 1 Microstructures of the as-received material and the annealed materials heat-treated at 500℃ 2h, 600℃ 3h, and 750℃ 2h, respectively.

To obtain the mechanical properties of the testing materials, the uniaxial tensile tests of the dog-bone-shape specimens with the thickness of 0.5, 1.0, and 1.5mm and various grain sizes were conducted following the standard of ASTM: E8/E8M. Two points were marked on the specimen so that an optical extensometer can measure the elongation of the specimen. The crosshead velocity of 2.1mm/min and the strain rate of $0.001s^{-1}$ were used. In each state with a given thickness and an average grain size, three repeated experiments were performed. The obtained stress-strain curves are illustrated in **Figs. 2** (a)~(c), and the dimensions of specimens are shown in **Fig. 2** (d).

The true stress is increased with the decrease of grain size in the same thickness, because the increasing grain boundaries prohibit the slip transfer among grains and further enhance the strength of the material and resistance of deformation. Moreover, the fracture strain is reduced with the increased grain size.

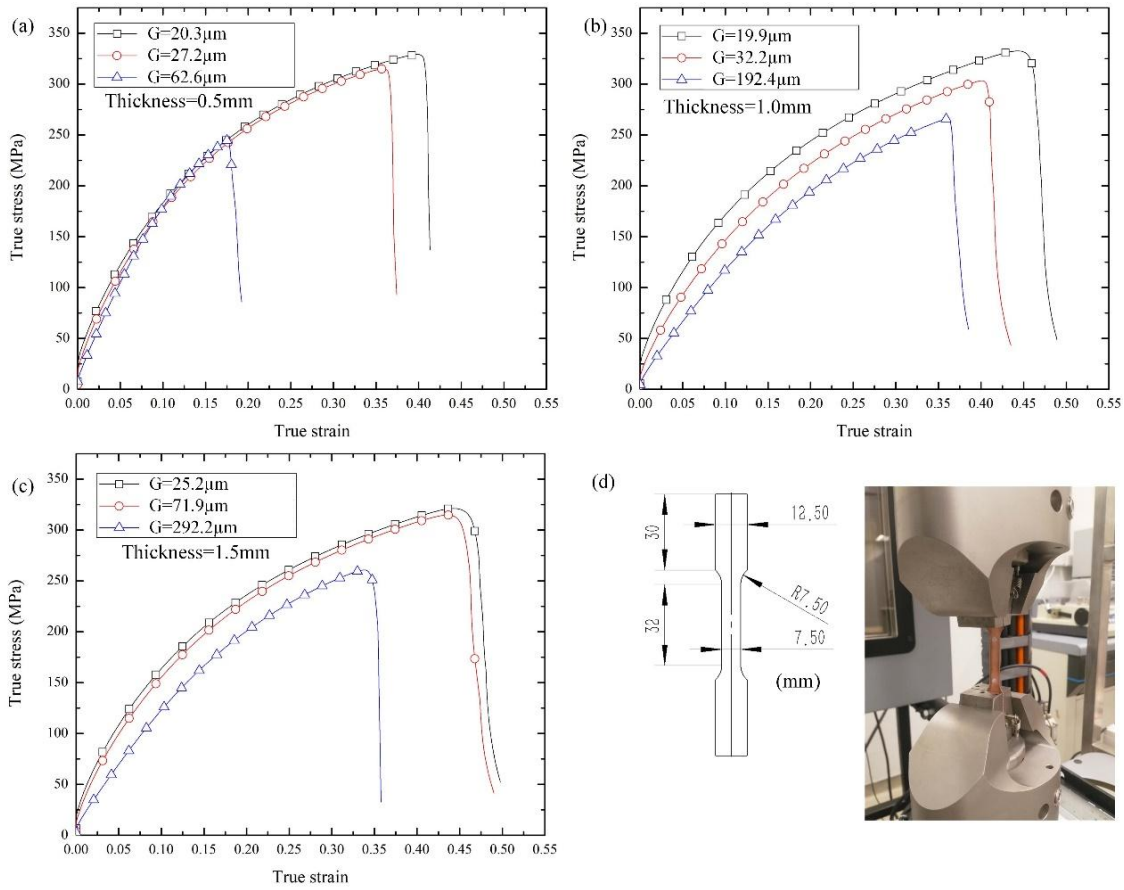

Fig. 2 Stress-strain curves of specimens in thickness of (a) 0.5mm; (b) 1.0mm; (c) 1.5mm, and (d) the test specimen.

2.2 Progressive forming system and the formed parts

The design and dimensions of the conical flanged part in three scales are shown in **Fig. 3** (a), and **Fig. 3** (b) shows a photo of the formed parts. In this study, the scaling factor (SF) is defined as the ratio of thickness of the specimen to one millimeter to represent the micro-scale, small meso-scale and large meso-scale, and it has the values of 0.5, 1.0 and 1.5 in this study. A forming system with three-scaled punches

and dies was developed and it contains four forming operations. The detailed designs and corresponding dimensions of the progressive tools and the four forming operations are illustrated in **Fig. 4**. Since the clearance affects the shearing process, the punch-die clearance in each side between punch and die with different scaling factors in punching and blanking operations are shown in **Table 1**. In this experiment, the pure copper sheets with the thickness of 0.5, 1.0, 1.5mm were used as specimens. The system uses different scaled punches and dies but the same blank holder. It is shown in **Fig. 4** that the specimen underwent a shearing deformation in the first forming operation, then a positioning hole was pierced, and a cylindrical part was blanked out. In the next step, the sheet metal was located by the positioning hole, then the material was extruded to flow into the conical cavity of the die until the spacing shoulder of the punch touched the upper surface of the material. In this operation, the outer conical surface of the flanged part was formed preliminarily. In the third operation, a truncated conical-shaped punch continuously pushed the material to be extruded in the thickness direction and the inner and outer conical surfaces of the flanged part were formed completely. The cylindrical hole feature was also fabricated after the third operation. Finally, the flanged part was ejected from the copper sheet by shearing deformation in the last step. The whole forming process was conducted with an MTS testing machine and the deformation load was measured by a 50kN maximum capacity load cell. Machine oil was used as lubrication on the interface to minimize the friction. The slow punch velocities of 0.003, 0.006 and 0.009mm/s were applied to the three pairs of punch and die, respectively. Due to the slow velocities employed, the strain rate effect in the forming processes could be ignored.

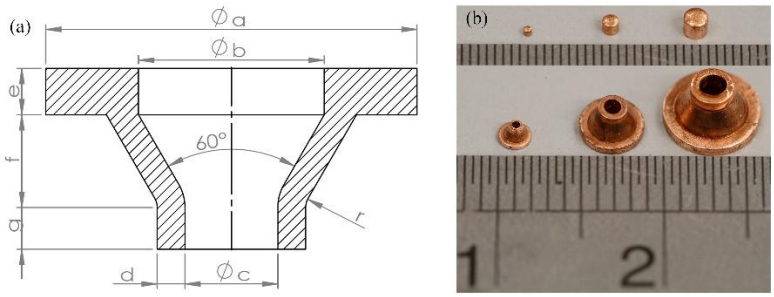

Scaling factor	Dimension (mm)							
	a	b	c	d	e	f	g	r
0.5	2	1	0.5	0.2	0.25	0.5	x	0.1
1	4	2	1	0.4	0.5	1	2x	0.2
1.5	6	3	1.5	0.6	0.75	1.5	3x	0.3

Fig. 3 (a) Designed dimensions of the flanged parts with three scaling factors and (b) formed parts.

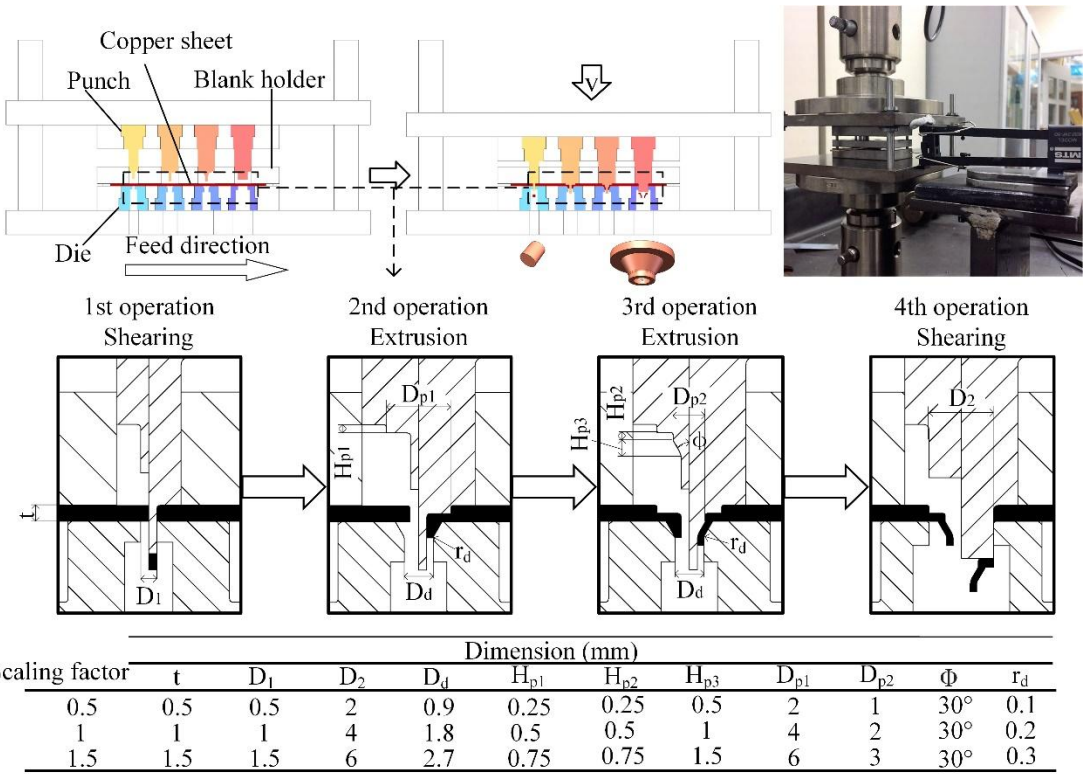

Scaling factor	Dimension (mm)										
	t	D_1	D_2	D_d	H_{p1}	H_{p2}	H_{p3}	D_{p1}	D_{p2}	Φ	r_d
0.5	0.5	0.5	2	0.9	0.25	0.25	0.5	2	1	30°	0.1
1	1	1	4	1.8	0.5	0.5	1	4	2	30°	0.2
1.5	1.5	1.5	6	2.7	0.75	0.75	1.5	6	3	30°	0.3

Fig. 4 Progressive microforming operations and dimensions of tooling.

Table 1 Clearance of each side between punch and die

Scaling factor / Step	0.5	1.0	1.5
Punching (1st)	0.011mm	0.010mm	0.003mm
Blanking (4th)	0.018mm	0.011mm	0.023mm

3. Results and discussions

3.1 Working pressure in deformation

The first and last operations in this progressive forming process can be recognized as micropunching and microblanking. Both are shearing operations, while microblanking is a method to fabricate bulk parts from metal strips while micropunching is used to produce microholes (Fu and Chan, 2014). The shearing process in progressive microforming has been systemically studied by previous researches. Xu et al. (2012) revealed the influence of grain and specimen size effects and blanking clearance on the ultimate shearing strength and fracture mechanism during shearing process. Fu and Chan (2013a) divided the shearing process into three stages according to flow stress and made a comparison among two forming systems with different grain sizes and scaling factors. Meng et al. (2015b) extensively investigated how lubricated conditions, punch-die clearance and shearing velocities affect the shearing process. On the other hand, the extrusion processes in previous researches were different from each other due to the various shapes of tooling and forming technologies. In this study, deformation behaviors in the extrusion processes with different scaling factors and grain sizes will be thoroughly discussed. **Figs. 5** and **6** reveal the relationship between forming pressure and the normalized stroke in the second and third operations with various material states, and the illustrations of two extrusion processes are shown in **Figs. 5** (d) and **6** (d). The terminologies of "forming pressure" and "normalized stroke" were defined to describe the ratio between the

immediate deformation load and the projection area of punch and the immediate stroke divided by the total stroke in each forming step. As shown in **Fig. 5**, the deformation curves of the second operation can be divided into two stages. In stage I, the workpiece is only pressed by the fillet of punch, and the stepped surface of punch does not fully press the material, so the curves present an increasing slope. In stage II, the punch presses the material until the stroke limit, and it presents a slight decreasing slope. The decreasing slope in this stage is due to the plastic deformation and the decrease of the length of shear band with punch stroke. For stage I, Chan and Fu (2013) revealed that when the size of rollover is less than the radius of punch fillet, there is a small gap which changes the initial tooling position of the forming operation and the size of rollover increases with the increased grain size. The influence of the size of rollover and the radius of fillet can be found in **Fig. 5** (b). When the fine-grained specimen (G=19.9μm) is applied, the size of rollover is smaller than the radius of fillet. The little gap between the stepped surface of punch and the material appears at the initial stage. However, for the coarse-grained materials (G=32.2μm and G=192.4μm), the size of rollover is larger than the radius of fillet. Therefore, the stepped surface of punch fully presses the material at the beginning of this operation and thus there is no stage I in the coarse-grained material. By comparison among all the scaling factors, the forming pressure decreases with the increased grain size, which could be elucidated by the mechanism of grain boundary strengthening. Moreover, the curve with the grain size of 192.4μm in the scaling factor of 1.0 is significantly lower than those of other scaling factors, which could be explained by the anisotropy of grain orientations due to the large grain size. By comparing the deformation curves among different scaling factors vertically, it is revealed that the forming pressure is smaller in the two meso-scaled progressive forming processes

than that in the micro-scaled process, which could be caused by the decreasing interfacial friction. Engel (2006) and Vollertsen et al. (2009) summarized the lubricant pocket model to explain the size effect affected interfacial friction in microforming, which can support the results of the experiments. In this theory, when scaled down to micro-scale, the surface of specimen has fewer lubricant pockets which can hold the lubricant to reduce friction, leading to worse interfacial lubrication.

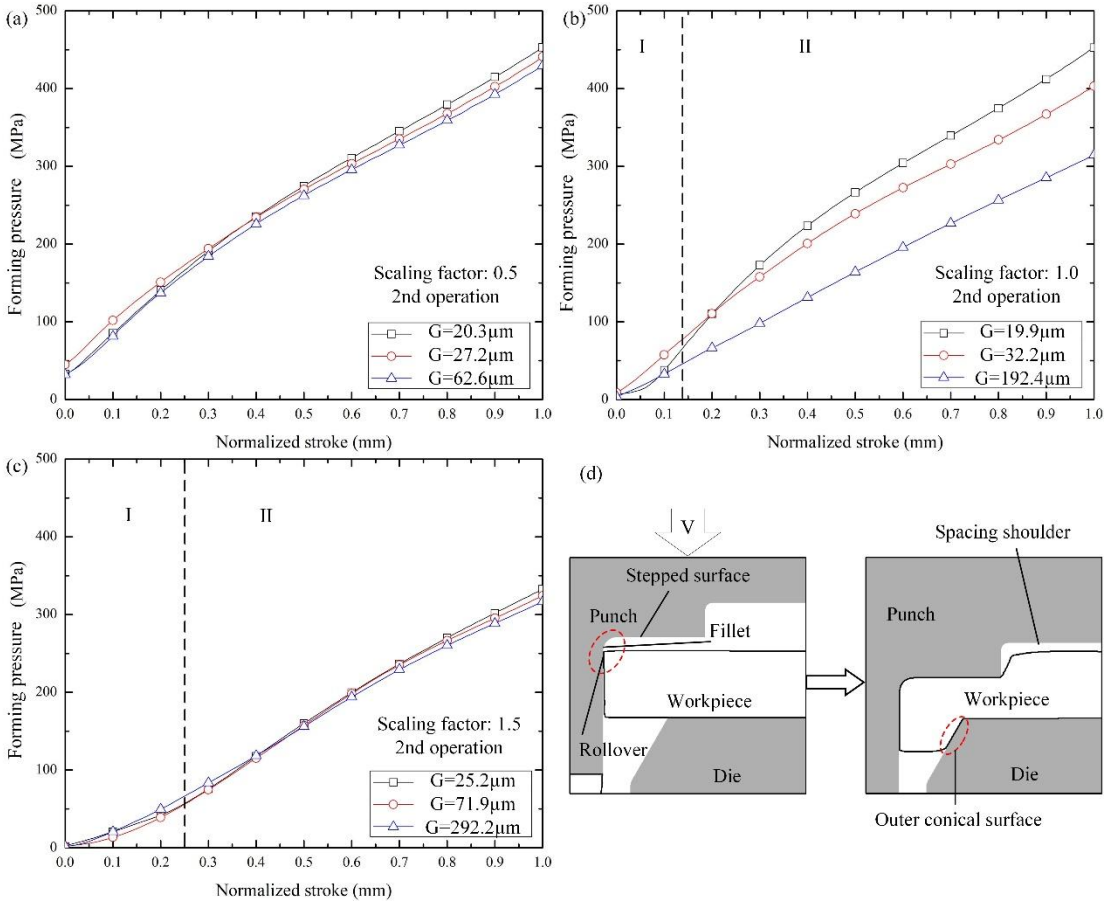

Fig. 5 The load-stroke curves and the schematic of the second forming step.

To further investigate the deformation behaviors in the third operation, the curves of forming pressure are shown in **Figs. 6** (a)~(c). According to the curves, the extrusion can be divided into four deformation stages, which are shown in **Fig. 6** (d), viz., elastic deformation, preforming deformation, wall-extrusion deformation, and

over-limit deformation. In stage I, the specimen is mainly subject to elastic deformation generated by the contact force between the fillet of punch and workpiece. The second stage begins when the conical surface of punch touches to the workpiece and finishes with the contact between the cylindrical surface of punch and the workpiece. In the second stage, the forming pressure is increased, which could be the results from the increase of working hardening, interfacial friction and the vertical projection area of contact surface between punch and the workpiece. The third stage is the deformation period when the cylindrical surface of punch contacts the workpiece. In this stage, the preformed outer conical surface of workpiece is pressed uniformly by the conical surface of the punch, generating a steady load-stroke curve. Moreover, stage III in these curves show a slightly increased slope induced by the increasing interfacial area of tooling and workpiece and the friction in between during the formation of the cylindrical hole feature. This slope is more obvious in micro-scale than that in meso-scale due to specimen size effect affected by the lubrication. After stages II and III, the material has been pressed to flow into the space between punch and die, and then the punch reaches the stroke limit and the forming pressure is increased rapidly when the spacing shoulder of the punch touches the workpiece, which is stage IV.

Meanwhile, the forming pressure is decreased when the grain size is increased for the grain boundary strengthening effect. By comparison among different scaling factors, the forming pressure is found to be decreased as the specimen size is increased to meso-scale. But the difference is not as obvious as that in the first extrusion since the interfacial friction and lubricant condition have only a little influence on this operation.

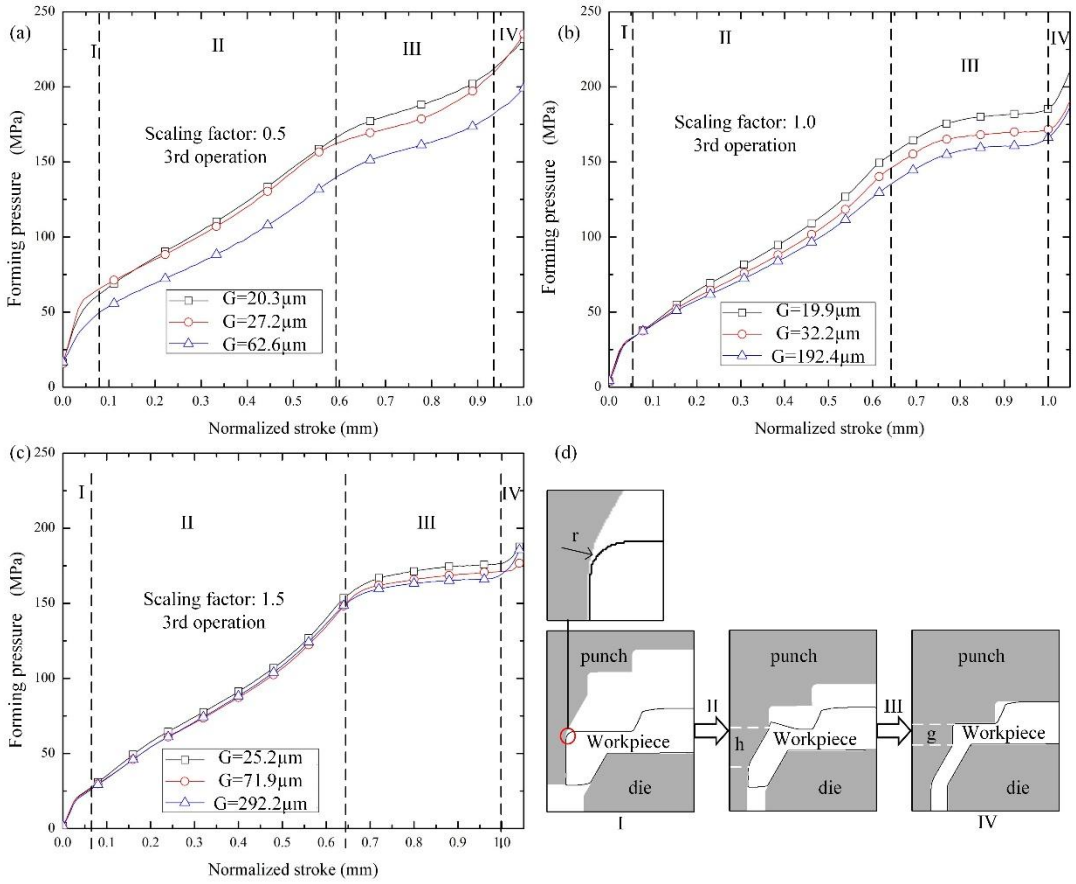

Fig. 6 The load-stroke curves and the schematic of the third forming step.

The comparison of the forming pressure-normalized stroke curves of the second and third extrusion operations with the three scaling factors and the approximate grain size are shown in **Fig. 7**. In both the extrusion operations, the forming pressure is decreased with the increase of scaling factor. In the second operation, as shown in **Fig. 7** (a), the forming pressure drops significantly when the scaling factor is increased to 1.5, which is due to the reduction of interfacial friction between the workpiece and tooling caused by the increased number of the close lubricant pockets (Engel, 2006). Furthermore, in the third operation as shown in **Fig. 7** (b), due to the decreasing interfacial friction, the deviation in the four steps is more obvious in meso-scale than that in micro-scale, which is useful for stroke control and accuracy control of the

dimensions in the deformed part. On the other hand, stroke control becomes more important when the forming system is scaled down to micro-scale, since the deviation of different steps in the forming operation is not as clear as that in meso-scale.

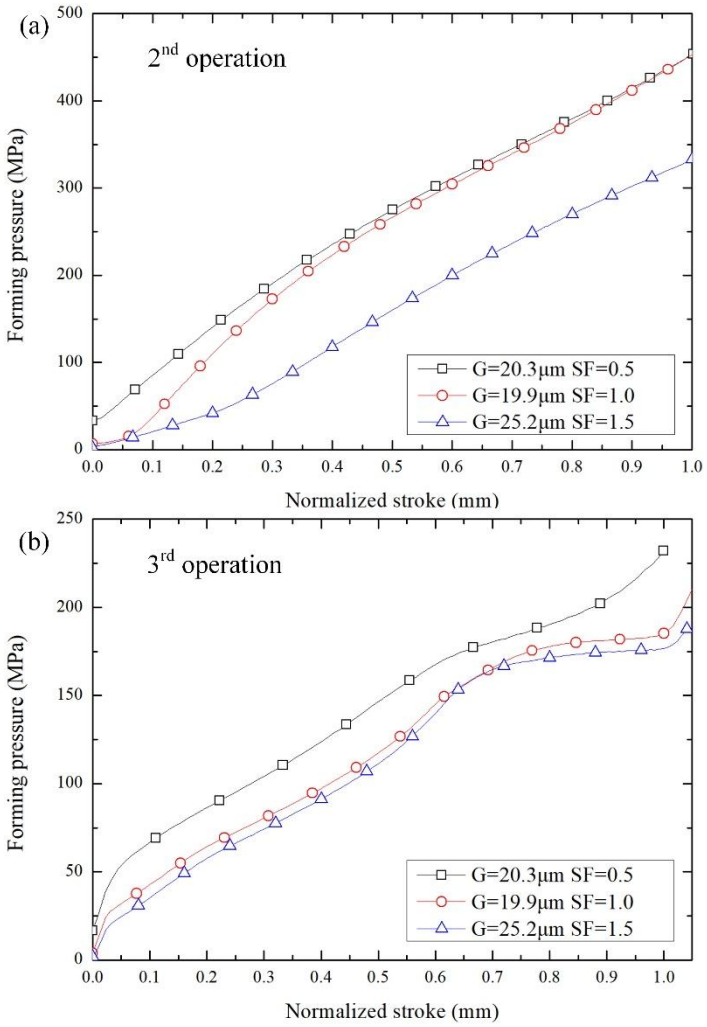

Fig. 7 The load-stoke curves with different scaling factors and approximate grain sizes in (a) 2nd operation; (b) 3rd operation.

3.2 The microstructure of fabricated part

The observation of microstructural evolution in the cross-sections of the progressively formed parts was conducted by an optical microscope after polishing

and etching. The sizes and lengths of features were measured based on the plotting scales shown on each photograph, respectively.

3.2.1 Cylindrical parts

In this research, three cylindrical parts were fabricated, and their scaled length were measured. **Fig. 8** (a) shows the microstructures of the blanked cylindrical parts and their corresponding scaled lengths are shown in **Fig. 8** (b). The ordinate scaled lengths is defined as the ratio between the billet length over the scaling factor. It is revealed from **Fig. 8** (a) that when the grain size increases, the length of the blanked cylindrical parts decreases and the shape of cylindrical parts becomes irregular for the workpiece with the same thickness, which also complies with the conclusion of Fu and Chan (2013a) and Meng et al. (2015b; 2018). This is because the anisotropic property of each single grain is enhanced when less grains are involved in the deformation, decreasing the homogeneousness of deformation and leading to discordance of the direction between grain slip and shearing. To further investigate the relationship between the length of blanked cylindrical parts and the specimen size, the scaled length was calculated as shown in **Fig. 8** (b). It can be found that the scaled length decreases with the decrease of specimen size, which is due to the increasing interfacial friction and lateral material flow. Therefore, the length of cylindrical parts is hard to meet the design requirement when the specimen size is scale down to micro-scale or the grain size is increased.

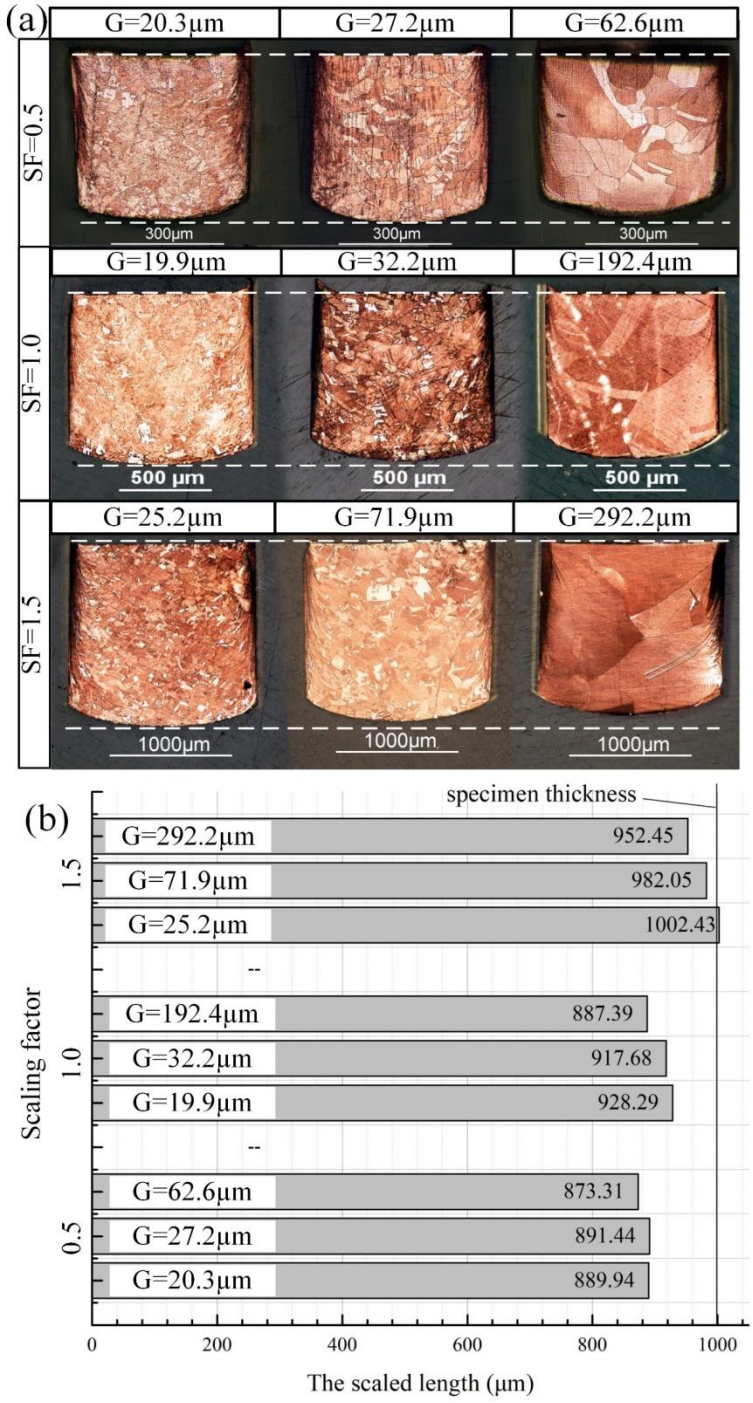

Fig. 8 (a) The microstructures and (b) the scaled length of cylindrical parts.

3.2.2 Conical flanged parts

Fig. 9 shows the observed microstructures with different material states. The microstructure on the cross-section along the diameter direction can be divided into

four zones in term of the flow lines and material deformation, viz. Zones I, II, III, IV. In these deformation zones, Zone I is the less-deformed area, which is referred to the "dead zone" and consistent with the findings by (Ghassemali et al., 2013a). There are three dead zones on the cross-section including two areas on the head-stepped feature which are divided by the shear band, and one on the cylindrical hole feature surrounded by Zone II. The areas of Zone I with different grain sizes are almost the same. Zone III is the area with a large extrusion. The grains in this area are elongated and rotated greatly, so the grain boundaries are thus indistinct. Zone III appears in the middle part of the conical feature, and its width decreases with the increase of grain size. In addition, Zone II is the transitional area between Zones I and III, in which the grains are slightly elongated, and their boundaries are distinct. Its area depends on the areas of Zones I and III. Zone IV, defined as the shear band, occurs in the head-stepped feature between the edges of punch and die, which is formed in the first extrusion operation. This band is narrow, and the transitional area is hard to be recognized. Furthermore, a small shear band can be found on the bottom burr near the hole of the flanged part, which is attributed to the shearing process of the first punching operation. The width of the shear band is increased, and it becomes more unrecognizable when the number of grains involved in the deformation decreases.

Ghassemali et al. (2013a) revealed that the entrance fillet radius of die improve the material flow toward the die cavity, which leads to a continuous deformed zone, and if there is no tooling fillet radius, the dead zone becomes shorter. In this study, nevertheless, there is no entrance fillet radius on the dies, so the large-deformed zones are incontinuous. As shown in **Fig. 9** (d), the grains near the edge of die is squeezed and narrow, which restrict the material flow between the two neighbouring areas. **Fig.**

9 (e) shows the detailed Zone III formed by the material with G=27.2μm, where the grains are elongated significantly, and the grain boundaries are indistinct.

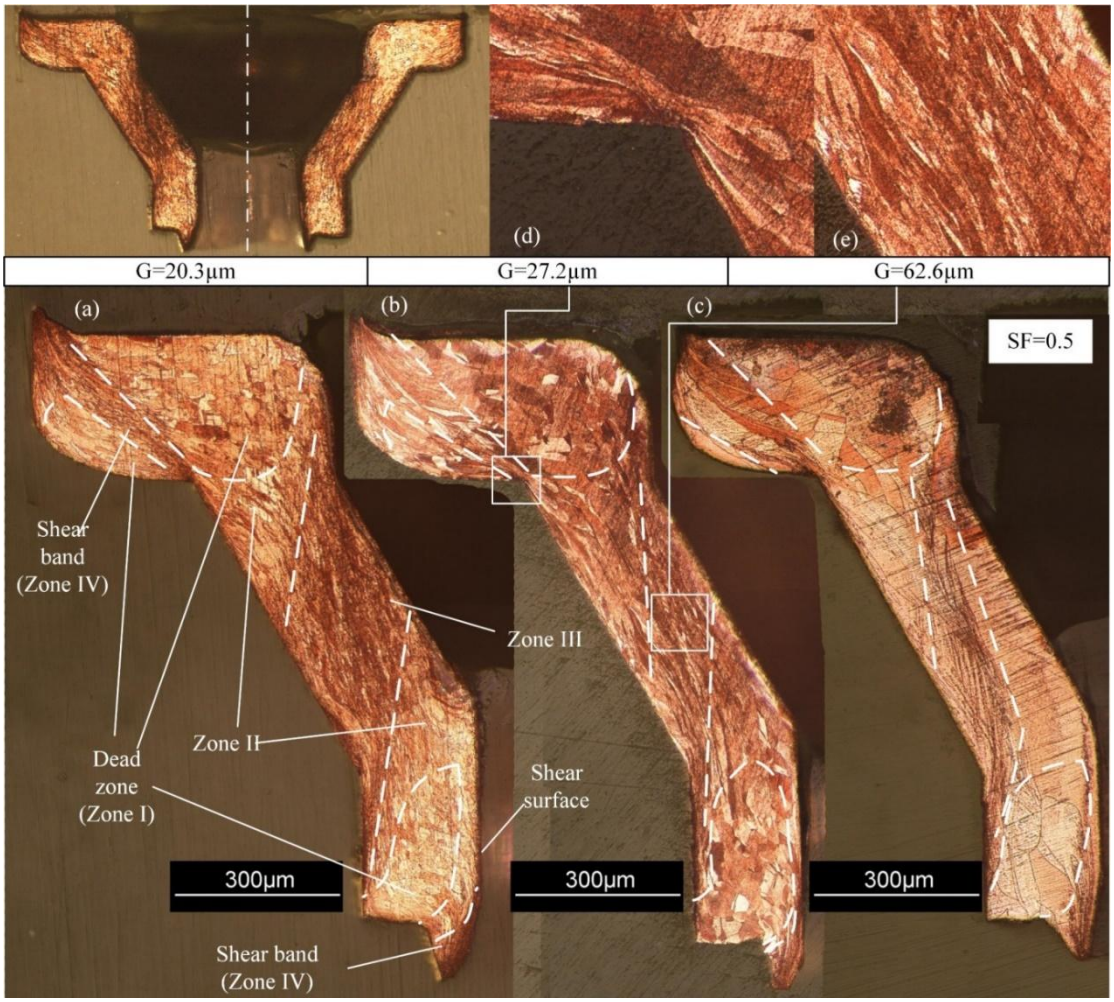

Fig. 9 Evolution of microstructure in the integrated micro-scaled flanged parts with different material states: (a) 500℃ annealed; (b) 600℃ annealed, (c) 750℃ annealed, (d) squeezed grains, and (e) elongated grains.

The microstructural evolution of the small meso- and large meso-scaled flanged parts with diverse grain sizes are shown in **Figs. 10** and **11**. The zone partition criterion of the micro-scaled flanged parts can also be applied to them. However, when the grain size increases largely compared to the part dimensions, as shown in

Figs. 10 (c) and **11** (c), only several grains are involved in the deformation, so the boundaries between different zones are indistinct. Moreover, the grain cracks in this case can be observed on the largely deformed grains, as shown in **Fig. 12**. This fracture phenomenon could be attributed to the high shear angle of single grains because only a few grains are involved in the deformation. Basson and Driver (2000) observed a shear band on a single crystal Cu during the large strain compression, which is similar to the phenomenon observed in this research.

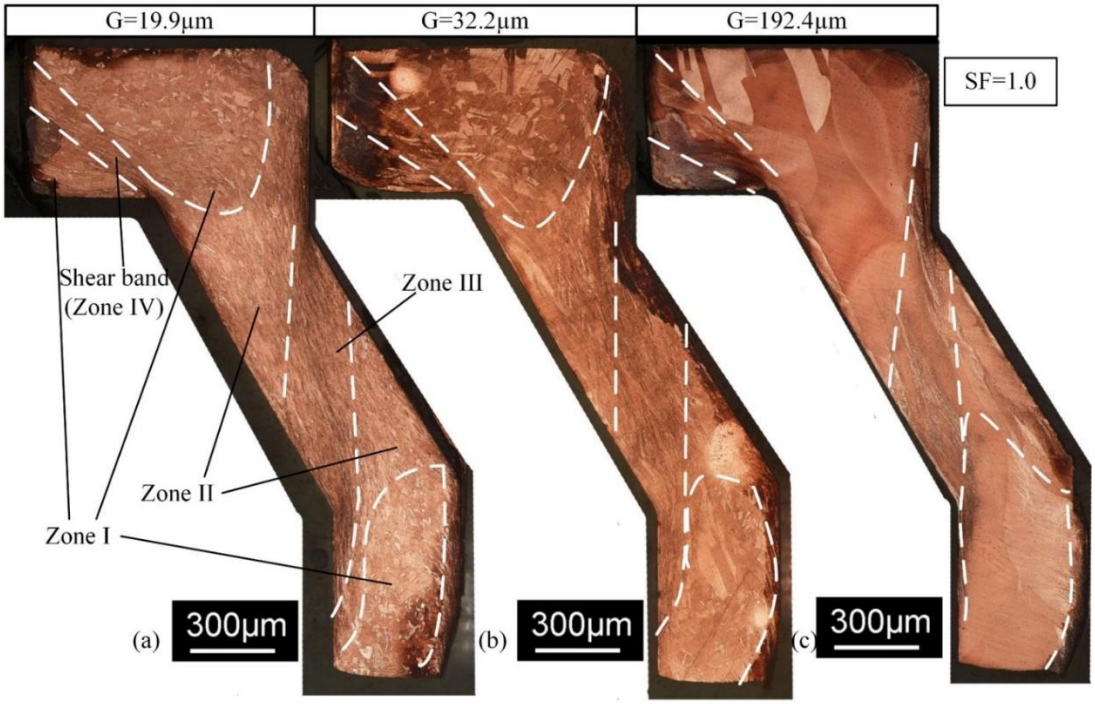

Fig. 10 Microstructural evolution in the small meso-scaled flanged parts with different material states: (a) 500℃ annealed; (b) 600℃ annealed, and (c) 750℃ annealed.

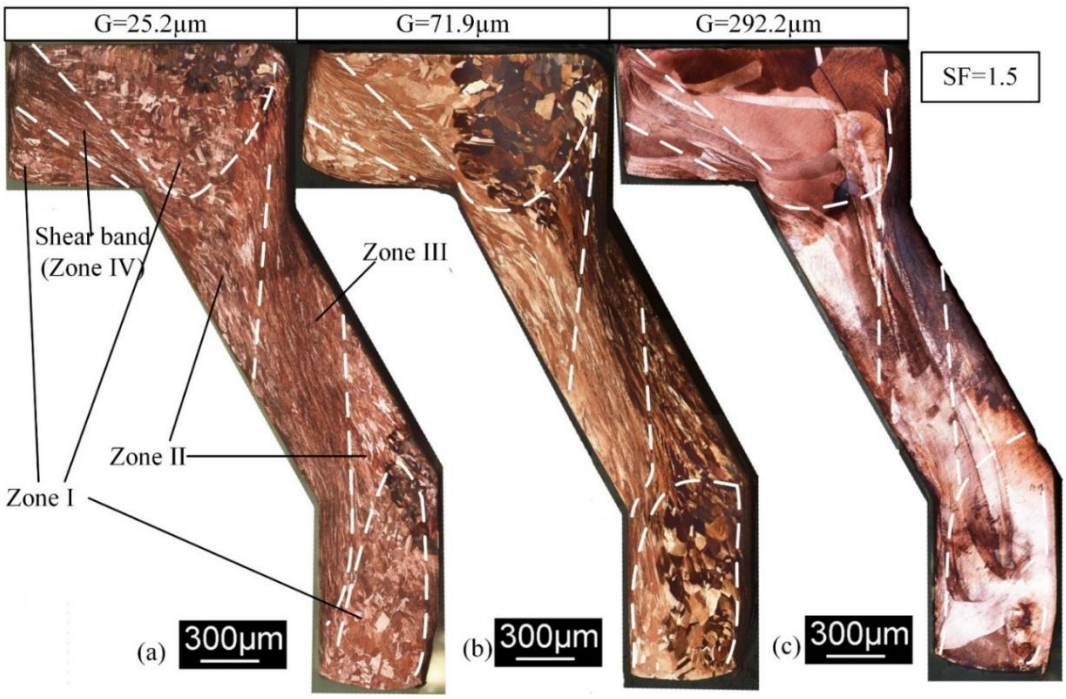

Fig. 11 Microstructural evolution in the large meso-scaled flanged parts with different material states: (a) 500℃ annealed; (b) 600℃ annealed, and (c) 750℃ annealed.

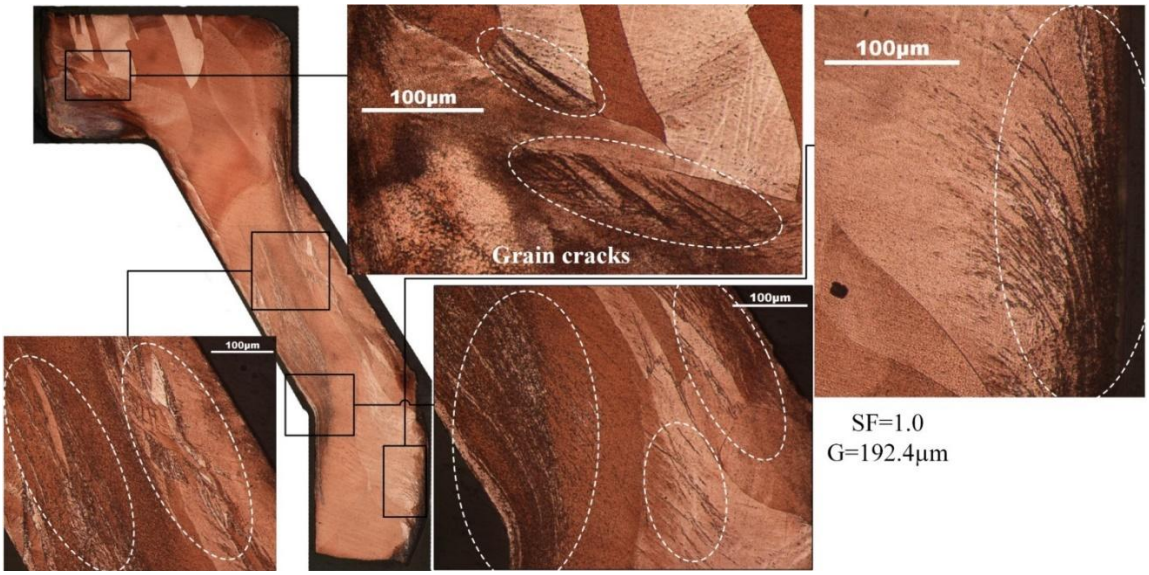

Fig. 12 Grain cracks in the small meso-scaled flanged part formed by the material annealed at 750℃.

3.3 Undesirable geometries

To investigate the distribution of undesirable geometries, the conical flanged part is divided into three features: the head-stepped feature (Feature A), the conical feature (Feature B), and the cylindrical hole feature (Feature C). The zone partition and the defects are illustrated in **Fig. 13**. In progressive microforming, undesirable geometries often appear on some specific areas, caused by strain accumulation, punch-die clearance, and shape of tooling. Feature A is produced by the second and the fourth operations, viz., extrusion and blanking operation. The undesirable geometries in this feature are primarily resulted from the blanking operation, as illustrated in **Fig. 14**. Burr and fracture usually occur on the sidewall of the blanked part after the shearing process, especially in the micro-scaled specimen due to size effect, which complies with the results in Meng et al.'s research (Meng et al., 2015a). However, the bottom of the compressed head-stepped feature has an inclination since there is no constraint applied to the bottom of the workpiece in the blanking operation. To achieve the desirable shape of the final formed part, a constraint on the inclined surface should be considered and employed in the blanking operation. The burr and inclination become worse in the micro-scaled parts attributed to the increasing interfacial friction. In addition, the rollover on the edge of the central hole is caused by the fillet of the third progressive punch. Furthermore, the bulge observed on medium grain size in small meso-scaled part could be caused by the bad lubricant condition in the return stroke. The shapes of Feature B are shown in **Fig. 15**. A desirable shape of this feature is obtained due to the complete constraints on both sides. The defects in Feature C are mainly the tail bulge, burr, and slope induced by the first and the third operations, as illustrated in **Fig. 16**. The shape of the cylindrical hole feature is attributed to multifactors including material flow, interfacial friction between workpiece and

tooling, and work hardening in shearing process. It can be seen from **Fig. 16** that the forming qualities of Feature C becomes deteriorated significantly in micro-scale, especially for the burr around the central hole, formed in the punching operation and accumulated in the final parts. In this forming scenario, the bottom surface of Feature C is a free surface. To improve the qualities of the final parts, a constraint should be employed and applied on this surface, which needs to be considered in tooling design.

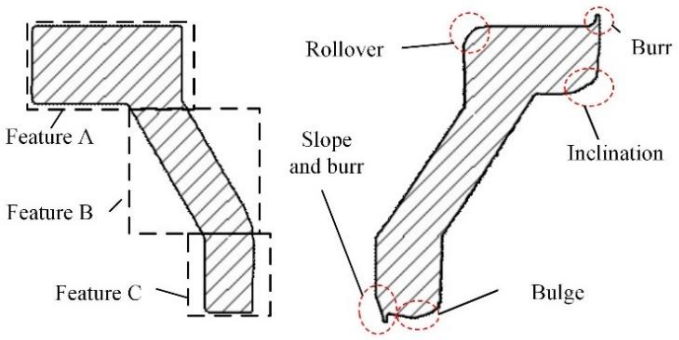

Fig. 13 The shape of the flanged part and its defects.

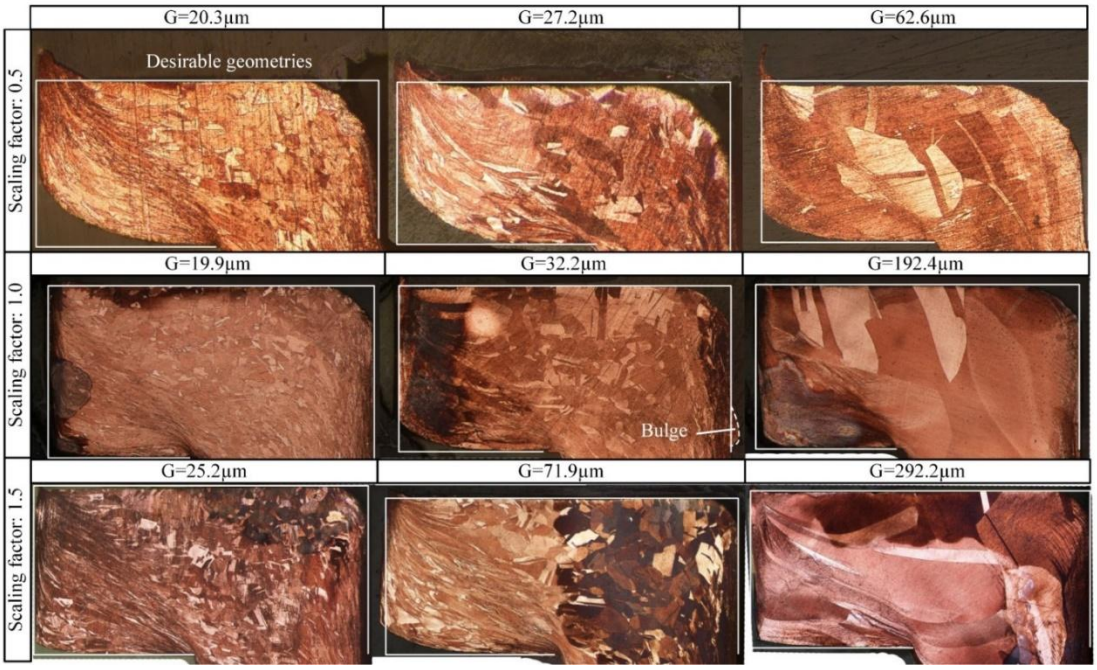

Fig. 14 Geometries of Feature A in different states.

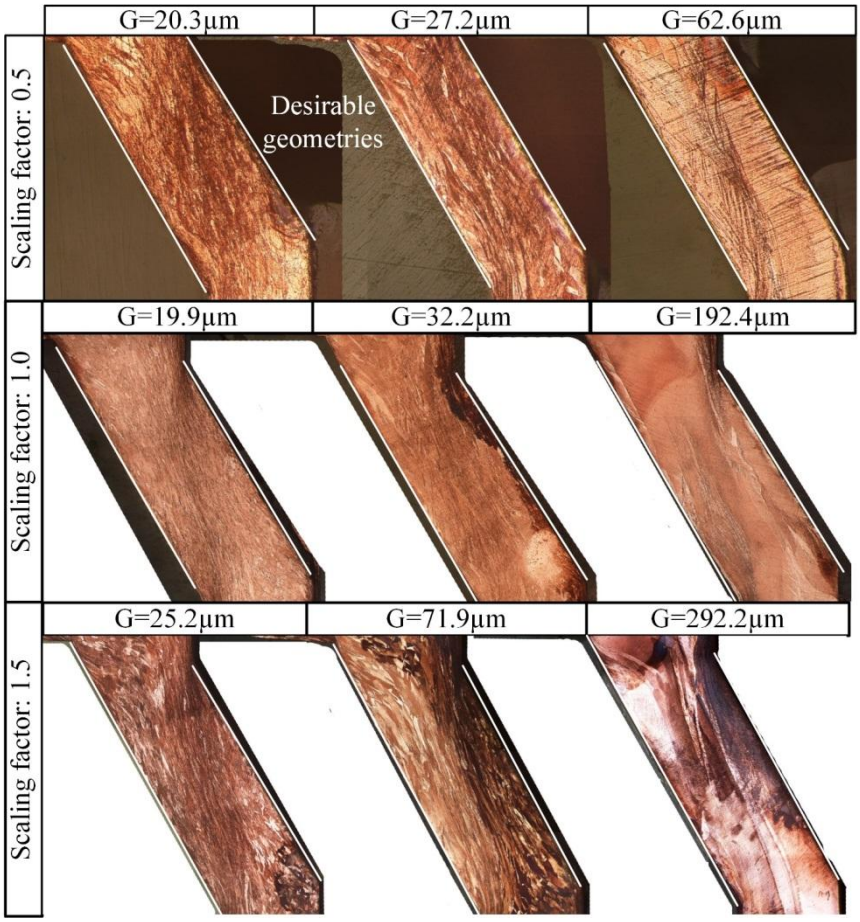

Fig. 15 Geometries of Feature B in different states.

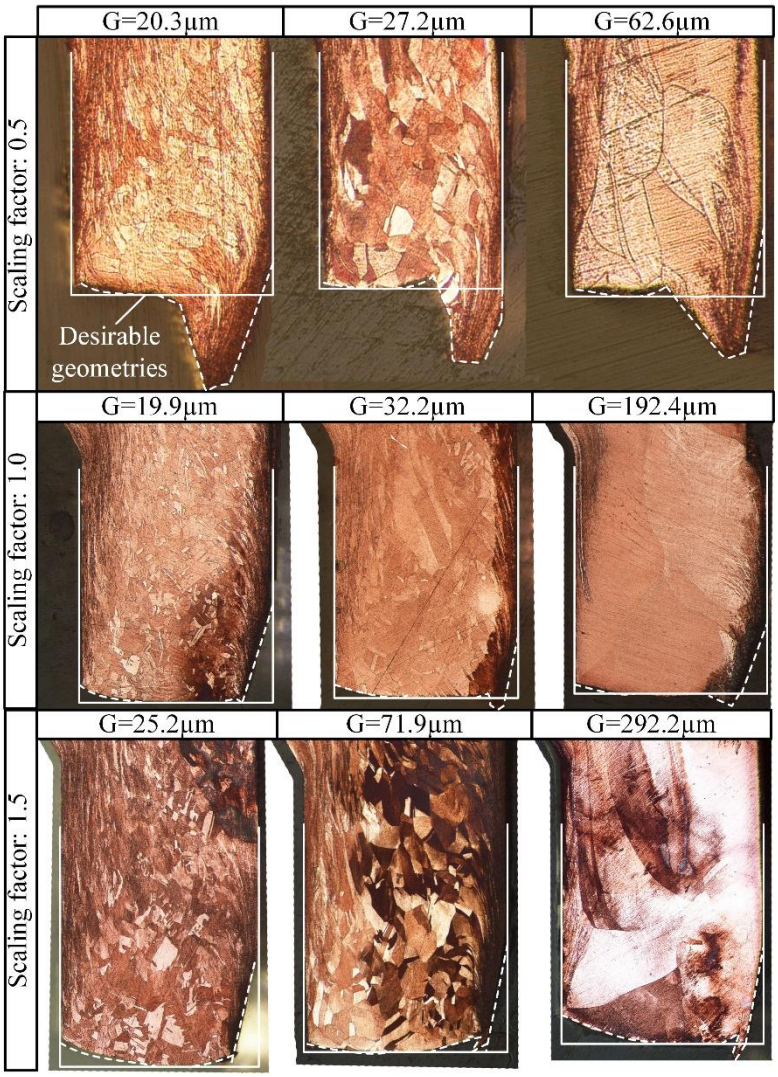

Fig. 16 Geometries of Feature C in different states.

To quantitatively investigate the specimen and grain size effect on the forming quality, the dimensions of the undesirable geometries on the formed features were analyzed numerically. In this research, four groups of dimensions were measured from both sides of the cross-section of two conical flanged parts in each material state and scaling factor. In the diagrams **Figs. 17** to **19**, the abscissa scaled length is defined as the length of feature divided by the scaling factor. **Fig. 17** shows the scaled length of undesirable geometries in Feature A with diverse scaling factors and grain sizes of

material. The deviation between the statistical dimension and designed dimension could be induced by the error in manufacturing process and measurement. It is revealed that the scaled length of the inclination increases with the decrease of grain size, which is induced by less grains involved in the deformation resulting in the inhomogeneous deformation and slip out of punch direction. The scaled length of the inclination is obviously increased with the decrease of scaling factor, since the formation of inclination is due to the interfacial friction between material and lateral side of die during the shearing process. As a result, a larger interfacial friction in the micro-scaled shearing process leads to a worse inclination. In addition, the scaled length of the burr increases with the decrease of scaling factor, but the trend is irregular within the same scaling factor. The regularity of the formation of burr in microblanking has been studied by Meng et al. (2015b) and Xu et al. (2012), which is affected by multifactors including punch-die clearance, lubricant condition, material thickness and grain size. **Fig. 18** shows the scaled length of the undesirable geometries on the cylindrical hole feature with different material conditions under the three scaling factors. The bulge is caused by interfacial friction between material and die. It can be found that the scaled lengths of bulges and the cylindrical hole features are generally reduced with the increase of grain sizes, since coarse-grained material leads to more inhomogeneous deformation and the property and orientation of single grain have more influence on material flow behavior. If the ideal homogenous material is applied, the shape of the tail cylindrical feature should be a parabolic shape if only affected by friction. When scaling factor decreases, the scaled length of bulge also decreases, owing to the increasing inhomogeneity. Moreover, **Fig. 19** shows that the scaled length of slopes is significantly increased in micro-scaled parts. The phenomenon of the slope observed on the cylindrical hole feature is generated by the

inhomogeneous material flow which is caused by work hardening in the first operation.

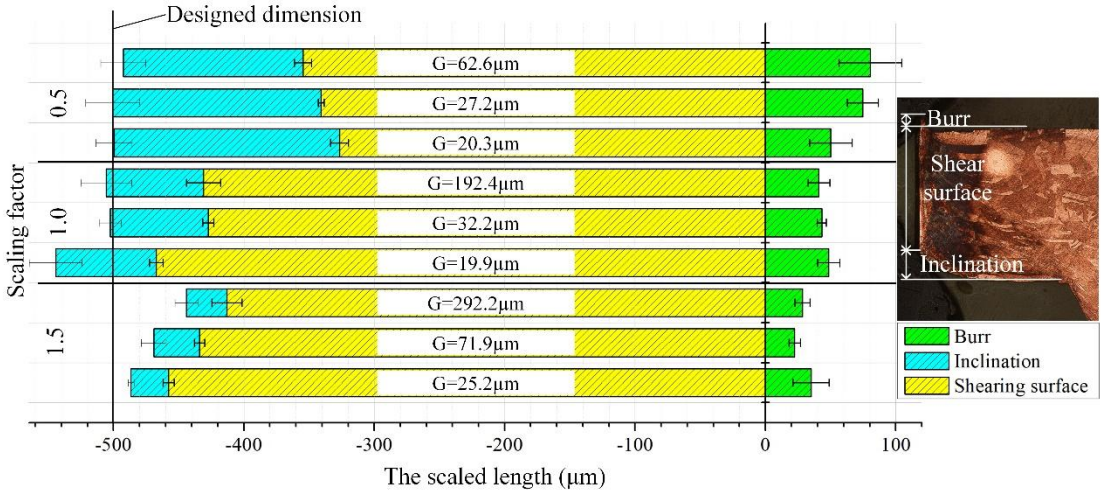

Fig. 17 Distribution of different geometries of the head stepped feature in various material conditions and scaling factors.

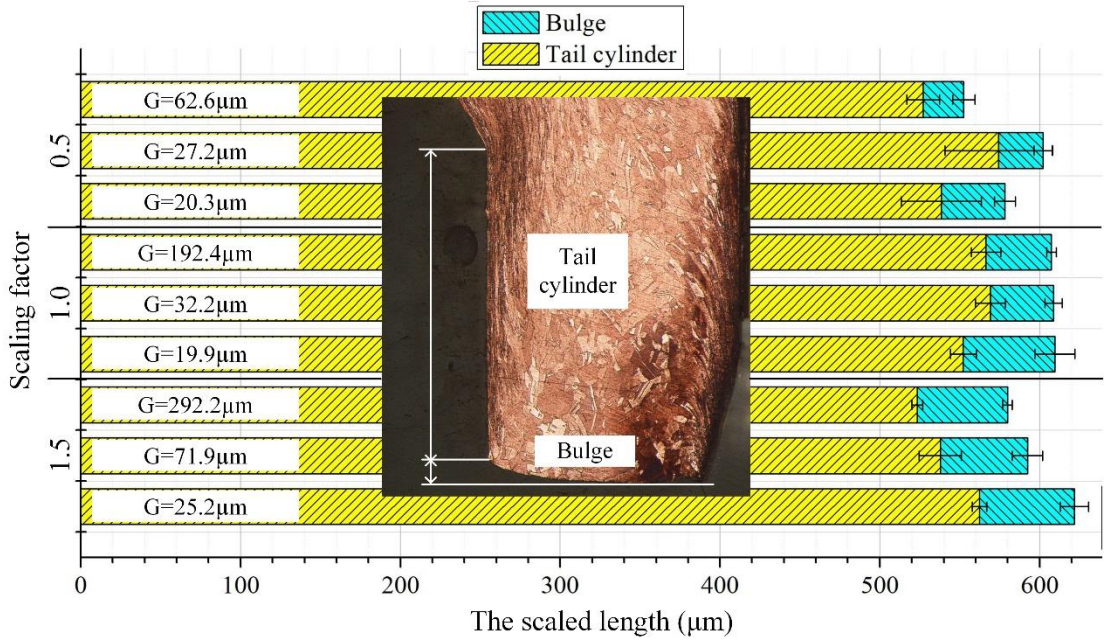

Fig. 18 Distribution of different geometries of the cylindrical hole feature in various material conditions and scaling factors.

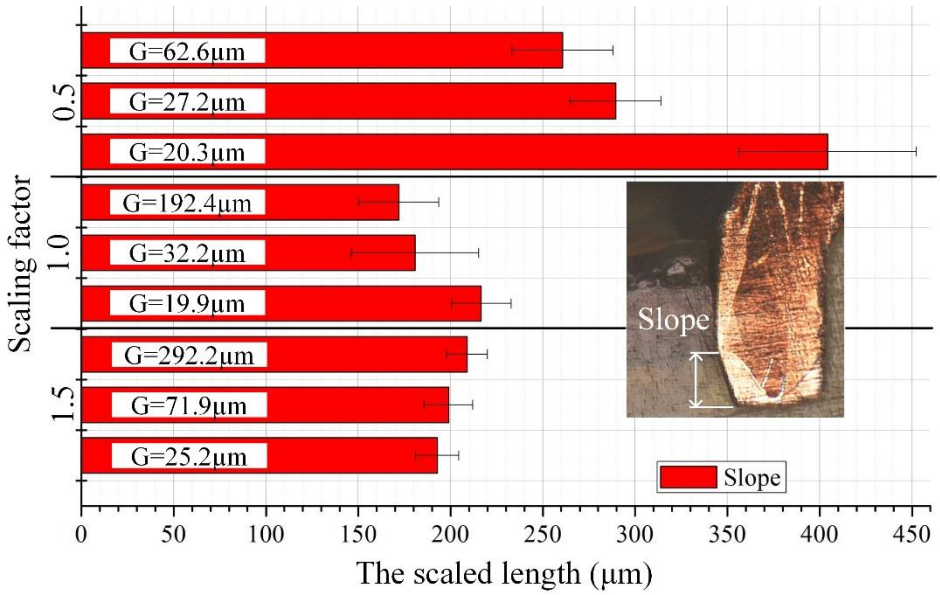

Fig. 19 The lengths of the slopes under different conditions.

3.4 Surface quality

The surface morphology of the conical surface of the flanged parts was observed by Scanning Electron Microscope (SEM). **Fig. 20** shows the surface morphology of the micro-scaled conical flanged part formed by the material annealed at 500℃, of which the grain size is 20.3μm. It can be found from **Fig. 20** (a), (b) and (d) that there are main two forming defects on the conical surface, viz. micro bulges and microcracks. A burr is observed on the edge of the central hole as shown in **Fig. 20** (c). On the other hand, the bottom surfaces of the cylindrical hole features have a good forming quality, and this phenomenon occurs similarly in different material states and scaling factors. This is because the conical feature of the part is under larger deformation in the extrusion operation compared with the bottom surface. Large deformation leads to more dislocations and anisotropy generated among various grains, which causes the deterioration of the conical surface. In **Fig. 21**, the stepped shoulder surface of the

micro-scaled flanged parts among different material states are compared. It is shown that dimples occur near the shearing surface of the blanking operation, and the number of them reduces with the increase of grain size, since fewer grains are involved in deformation. Meng et al. (2015a) indicated the fracture mechanism of dimples is attributed to the initiation, growth and coalescence of microvoids, which can only form at the grain boundaries or inclusions. **Fig. 22** shows the surface morphology of the small meso-scaled conical flanged part with the material annealed at 500℃, of which the grain size is 19.9μm. **Figs. 22** (b), (c) and (d) show the undesirable defects on the conical surface, where the micro cracks disappear and micro pits and fissures occur when the size of parts increases to meso-scale, and micro bulges still occur. **Fig. 22** (a) shows the burr on the edge of the hole, which is smaller than that in micro-scaled part. By comparing the forming qualities of micro-scaled and meso-scaled parts, it is revealed that the burrs on the central hole are significantly reduced in meso-scale and the defect characteristic changes. Therefore, for achieving a better forming quality of the micro-scaled conical flanged parts, a subsequent polishing process should be considered.

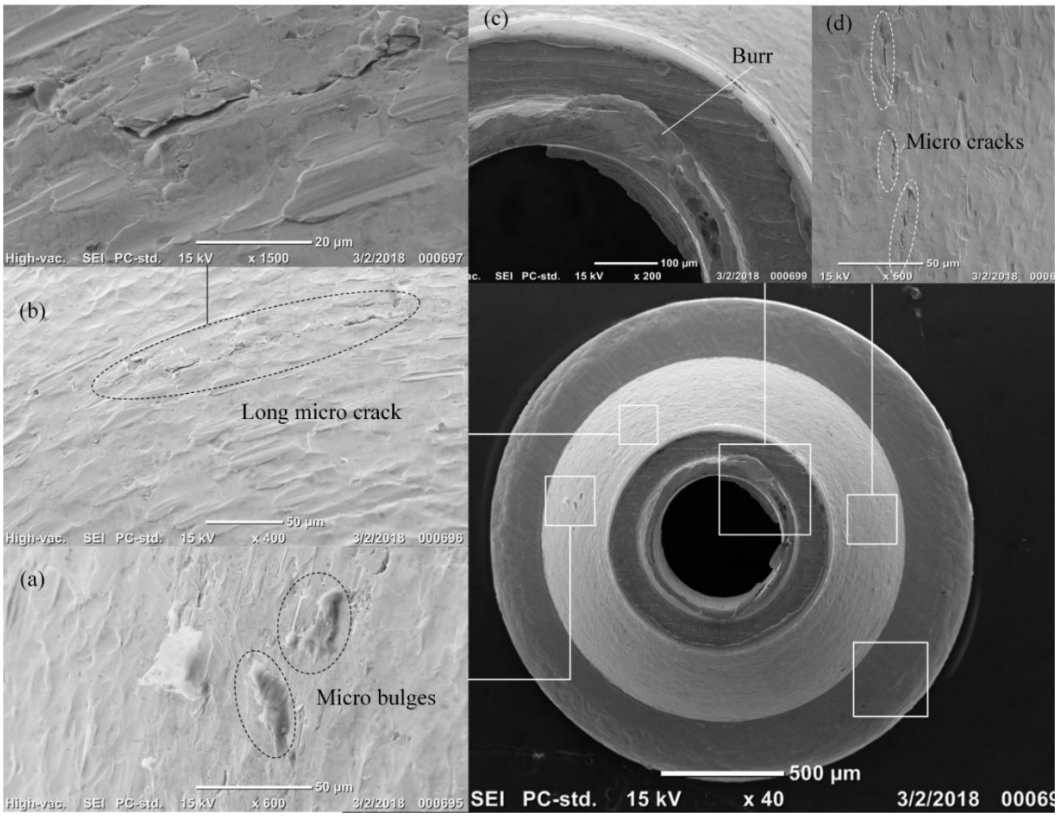

Fig. 20 SEM pictures of the part formed using 500℃ annealed material with the scaling factor of 0.5 (G=20.3μm).

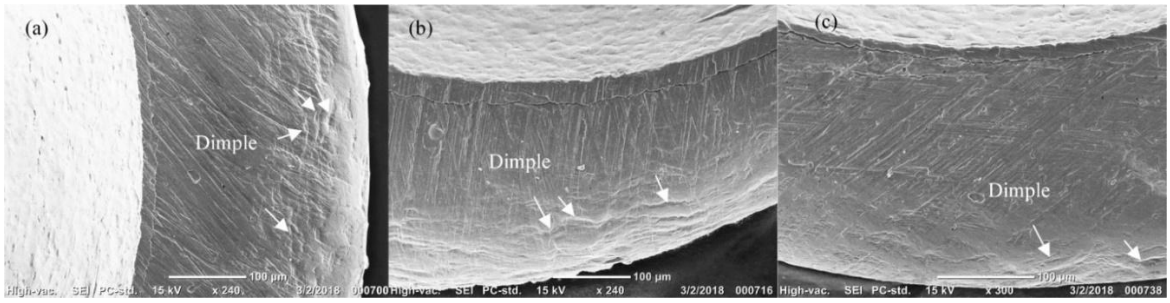

Fig. 21 SEM pictures of shoulder surface of head-stepped features with the scaling factor of 0.5 and the grain size of (a) 20.3μm; (b) 27.2μm; and (c) 62.6μm.

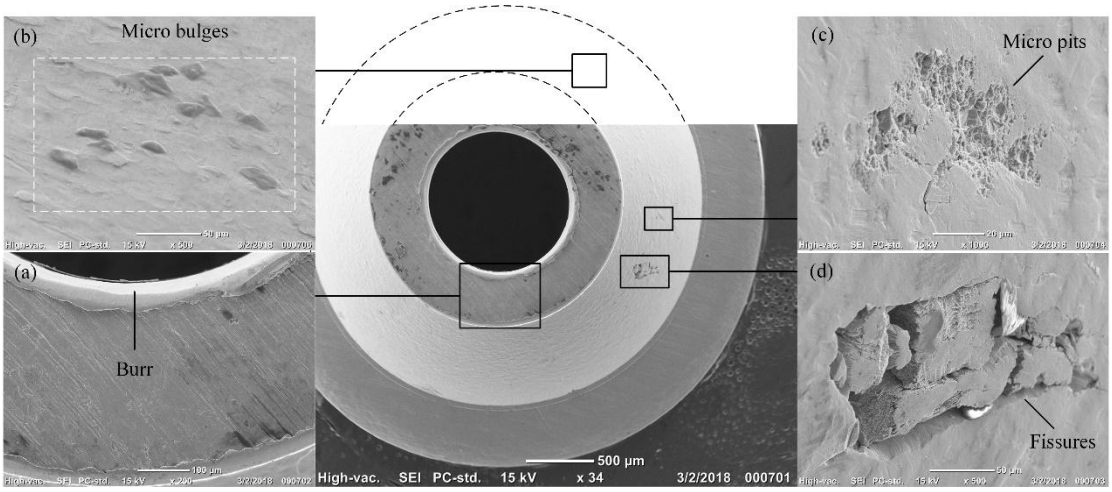

Fig. 22 SEM pictures of the part formed using the material annealed at 500℃ with the scaling factor of 1.0 (G=19.9μm).

To further study the influence of size effect on surface quality, the comparison of the outer conical surface among micro-, small meso- and large meso-scaled flanged parts was made as shown in **Fig. 23**. It is found that the density of the fish-scale patterns slightly increases with coarse-grained material. When the grain size is large compared to the specimen size, there are several grains exist along the wall thickness direction, thus the anisotropy of individual grain becomes significant and the random distribution of grains in material is declined, where inhomogeneous deformation happens. Moreover, when the size of parts is increased to large meso-scale, the forming quality of part surface is improved greatly. In microparts, the main defect on the conical surface is micro crack, resulting from strain accumulation in extrusion operation. Meanwhile, on the conical surfaces of small and large meso-scaled parts, micro pits are observed, but its formation mechanism needs to be further investigated. Different from the fine-grained material with scaling factor 1.0, micro cracks can also be observed on the conical surface with coarse-grained material.

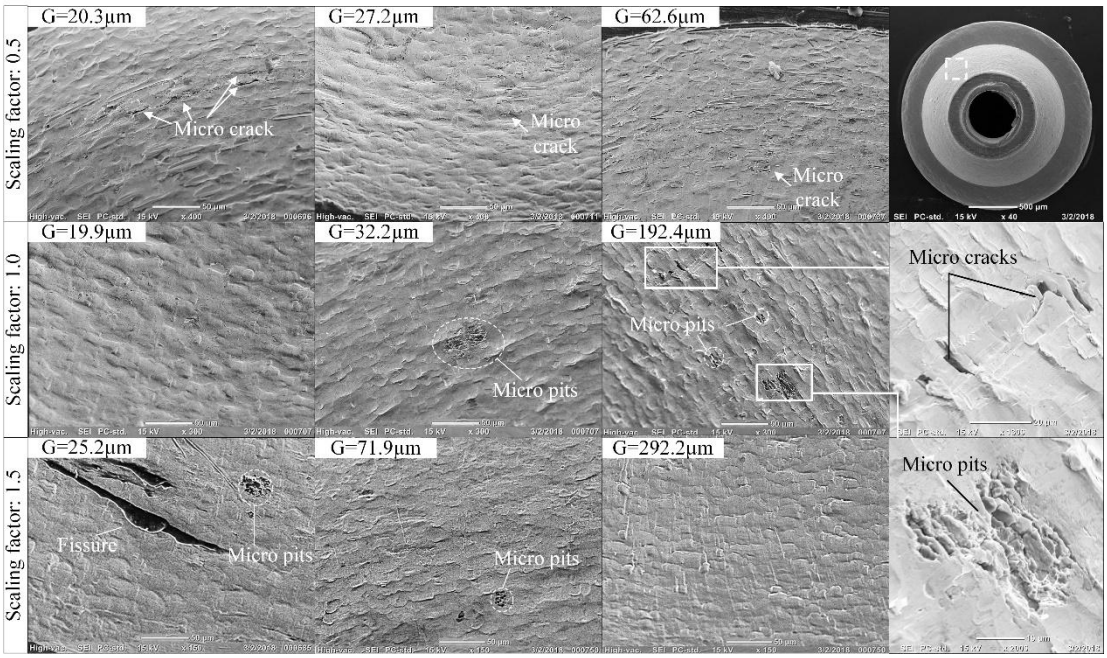

Fig. 23 SEM pictures of the conical surfaces with different scaling factors and materials states.

4. Conclusions

In this research, progressive formed conical flanged parts in three scales were fabricated by directly using sheet metals. The forming process was investigated from several aspects including forming pressure, evolution of microstructure, undesirable geometries, and fracture phenomenon. The following conclusions can be drawn from this study.

(1) The extrusion operation can be divided into several stages (the second operation can be divided into two stages and the third operation can be divided into four stages) according to the shapes of tooling and workpiece and their relative position represented by forming pressure-normalized strokes curves. The forming pressure of the progressive microforming process decreases with the increase of grain size, and increases when the part is scaled down from meso- to micro-scale. By the analysis of

forming pressure-normalized strokes curves and the corresponding deformation stages in each forming step, more accurate stroke control of punch can be achieved, which is useful in tooling protection and dimension accuracy assurance.

(2) The microstructures on the cross-section along the symmetry axis of the conical flanged part can be divided into four zones based on the deformed texture, and the boundaries of different zones become blurry with the increase of grain size. Moreover, the widths of Zones II and IV increase and the width of Zone III decreases with the increasing grain size.

(3) The scaled lengths of the cylindrical parts decrease with the decrease of scaling factor. The scaled lengths of inclination, bulge, head-stepped feature, and cylindrical hole feature decrease with the increased grain size in the three scaling factors. All the undesirable geometries except bulge in microparts become worse compared with those in meso-scaled parts. In addition, the undesirable geometries are easier to occur on the head-stepped and cylindrical hole features in micro-scale.

(4) The surface quality of the fabricated conical flanged parts is affected by grain and specimen sizes. The conical surface quality becomes significantly worse due to the large deformation in extrusion operations. Moreover, the forming quality shows a deteriorating tendency with the decreased specimen size and the increased grain size. Several typical defects can be observed on the conical surface, including micro bulges, micro cracks in micro-scale, and micro pits and fissures in meso-scale.

(5) The relatively coarse grains facilitate the forming of desirable geometries and reduce dimples on the shearing surface, but slightly deteriorate the conical surface quality. However, the overlarge grain size can result in grain cracks, which could reduce the strength of the deformed parts. In addition, constraints need to be applied

on the head-stepped and cylindrical hole features to improve the quality of shapes and geometries of microparts.

Acknowledgments

The authors would like to acknowledge the funding support to this research from the project of 152792/ 16E (B-Q55M) from the General Research Fund of Hong Kong Government and the project of No. 51575465 from the National Natural Science Foundation of China.

References

Basson, F., Driver, J.H., 2000. Deformation banding mechanisms during plane strain compression of cube-oriented f.c.c. crystals. Acta Mater. 48, 2101-2115.

Chan, W.L., Fu, M.W., 2013. Meso-scaled progressive forming of bulk cylindrical and flanged parts using sheet metal. Mater Design. 43, 249-257.

Cheng, T.C., Lee, R.S., 2018. The influence of grain size and strain rate effects on formability of aluminium alloy sheet at high-speed forming. J Mater Process Tech. 253, 134-159.

Engel, U., 2006. Tribology in microforming. Wear. 260, 265-273.

Engel, U., Eckstein, R., 2002. Microforming - from basic research to its realization. J Mater Process Tech. 125, 35-44.

Fu, M.W., Chan, W.L., 2013a. Micro-scaled progressive forming of bulk micropart via directly using sheet metals. Mater Design. 49, 774-783.

Fu, M.W., Chan, W.L., 2013b. A review on the state-of-the-art microforming technologies. Int J Adv Manuf Tech. 67, 2411-2437.

Fu, M.W., Chan, W.L., 2014. Micro-scaled products development via microforming. Springer series in advanced manufacturing Springer, London doi. 10, 978-971.

Gao, Z., Peng, L., Yi, P., Lai, X., 2015. Grain and geometry size effects on plastic deformation in roll-to-plate micro/meso-imprinting process. J Mater Process Tech. 219, 28-41.

Geiger, M., Kleiner, M., Eckstein, R., Tiesler, N., Engel, U., 2001. Microforming. Cirp Ann-Manuf Techn. 50, 445-462.

Ghassemali, E., Jarfors, A.E.W., Tan, M.J., Lim, S.C.V., 2013a. On the microstructure of micro-pins manufactured by a novel progressive microforming process. Int J Mater Form. 6, 65-74.

Ghassemali, E., Tan, M.-J., Wah, C.B., Lim, S.C.V., Jarfors, A.E.W., 2015. Effect of cold-work on the Hall–Petch breakdown in copper based micro-components. Mech Mater. 80, 124-135.

Ghassemali, E., Tan, M.J., Jarfors, A.E.W., Lim, S.C.V., 2013b. Progressive microforming process: towards the mass production of micro-parts using sheet metal. Int J Adv Manuf Tech. 66, 611-621.

Hirota, K., 2007. Fabrication of micro-billet by sheet extrusion. J Mater Process Tech. 191, 283-287.

Kim, G.Y., Ni, J., Koc, M., 2007. Modeling of the size effects on the behavior of metals in microscale deformation processes. J Manuf Sci E-T Asme. 129, 470-476.

Lin, B.-T., Huang, K.-M., Kuo, C.-C., Wang, W.-T., 2015. Improvement of deep drawability by using punch surfaces with microridges. J Mater Process Tech. 225, 275-285.

Meng, B., Fu, M.W., Fu, C.M., Chen, K.S., 2015a. Ductile fracture and deformation behavior in progressive microforming. Mater Design. 83, 14-25.

Meng, B., Fu, M.W., Fu, C.M., Wang, J.L., 2015b. Multivariable analysis of micro shearing process customized for progressive forming of micro-parts. Int J Mech Sci. 93, 191-203.

Meng, B., Fu, M.W., Shi, S.Q., 2018. Deformation characteristic and geometrical size effect in continuous manufacturing of cylindrical and variable-thickness flanged microparts. J Mater Process Tech. 252, 546-558.

Ran, J.Q., Fu, M.W., Chan, W.L., 2013. The influence of size effect on the ductile fracture in micro-scaled plastic deformation. Int J Plasticity. 41, 65-81.

Vollertsen, F., Biermann, D., Hansen, H.N., Jawahir, I.S., Kuzman, K., 2009. Size effects in manufacturing of metallic components. Cirp Ann-Manuf Techn. 58, 566-587.

Wang, J.L., Fu, M.W., Shi, S.Q., 2017. Influences of size effect and stress condition on ductile fracture behavior in micro-scaled plastic deformation. Mater Design. 131, 69-80.

Xu, J., Guo, B., Wang, C.J., Shan, D.B., 2012. Blanking clearance and grain size effects on micro deformation behavior and fracture in micro-blanking of brass foil. Int J Mach Tool Manu. 60, 27-34.

Xu, Z., Peng, L., Bao, E., 2018. Size effect affected springback in micro/meso scale bending process: Experiments and numerical modeling. J Mater Process Tech. 252, 407-420.

Zhang, H., Dong, X., 2016. Experimental and numerical studies of coupling size effects on material behaviors of polycrystalline metallic foils in microscale plastic deformation. Materials Science and Engineering: A. 658, 450-462.